

Discovery of Autophagy-Inducing Chloroquine Analogs with Potent Anticancer Activity in Breast Cancer Cells

Yasser Heikal^{1*}, Dhvani Patel^{1,2}, Peter Cao¹, Catherine C. Lincourt², Ashley O'Leary¹ and Dominic L. Ventura²

¹Department of Pharmaceutical, Social and Administrative Sciences, School of Pharmacy, D'Youville College, 320 Porter Ave., Buffalo, NY 14201, USA

²Department of Chemistry, School of Arts, Science and Education, D'Youville College, 320 Porter Ave., Buffalo, NY 14201, USA

Abstract

Targeting autophagy in cancer has emerged as a promising strategy for drug discovery. Autophagy is a conserved process required for the degradation and recycling of damaged organelles and proteins. Dysregulation of autophagy has been implicated in many diseases including cancer. In breast cancer, studies have demonstrated that activated autophagy promotes cell survival and therapeutic resistance. Chloroquine (CQ), an antimalarial and anti-inflammatory agent, has emerged as a potential anticancer agent due to its autophagy inhibitory activity; however, it lacks specificity and potency. In this study, we report the synthesis and evaluation of several CQ analogs. Interestingly, the most potent compounds identified 5 and 6, induced autophagy, as they enhanced the accumulation of LC3B-II and induced p62 protein degradation. Co-treatment of MDA-MB-231 cells with compound 5 and bafilomycin A1, an autophagy inhibitor, resulted in blocking apoptosis induction concomitant with partial rescue of cell viability, suggesting induction of autophagy-dependent apoptosis.

Keywords: Autophagy • Chloroquine • Breast cancer • Apoptosis

Introduction

Targeting autophagy has emerged as a promising strategy to develop novel therapeutic approaches for cancer treatment [1,2]. Dysregulation of autophagy has been implicated in many disease conditions including metabolic disorders, neurodegenerative diseases and cancer [3,4]. The role of autophagy in cancer remains controversial. Earlier studies in breast cancer have demonstrated that autophagy could play protective role against cancer development by mitigating genomic damage and metabolic stress [5]. However, accumulating body of literature implicates autophagy activation in cancer resistance to various therapeutic modalities [2]. Autophagy inhibition in breast cancer has been shown to enhance the efficacy of chemotherapy [6], HER2 receptor inhibitors [7], CDK4 inhibitors [8], estrogen receptor antagonists [9] and radiation therapy [10]. Additionally, studies have demonstrated that autophagy is involved in the maintenance of breast cancer stem cells [11]. Under nutrient rich conditions, constitutively active autophagy has been shown to activate STAT3 pathway in triple-negative breast cancer (TNBC) cells which results in inhibition of the apoptotic machinery [12]. Inhibition of autophagy in TNBC cells resulted in selective induction of apoptotic cell death [12]. The discovery of potent autophagy modulators could lead to the development of effective therapeutic modalities for the treatment of breast cancer. Conversely, studies suggest that autophagy induction could play a role in cell death [13]. A study by Luna-Dulcey et al. [14] demonstrated that autophagy induction in TNBC cells could induce apoptotic cells death. Additionally, accumulating evidence suggests that autophagy induction could induce apoptosis-independent cell death modalities such as autosis [15,16].

Chloroquine (CQ), a Food and Drug Administration (FDA)-approved drug for the treatment of malaria, rheumatoid arthritis and lupus erythematosus has emerged as a potential anticancer agent due to its ability to inhibit autophagy [17]. The mechanism of autophagy inhibition by CQ involves

inhibition of lysosomal acidification, which disrupts autophagy by preventing autophagosome fusion and degradation. A recent study by Mauthe et al. suggests the CQ inhibits autophagy by decreasing autophagosome-lysosome fusion [17]. Several ongoing clinical trials are currently evaluating CQ and/or hydrochloroquine as potential anticancer agents in combination with other therapeutic modalities [18]. However, several hurdles may prevent successful translation of CQ into the clinic. The CQ dose needed to inhibit autophagy *in vitro* is relatively high and may not be achieved clinically. Therefore, the observed clinical effects of CQ could be mediated by autophagy-independent mechanisms. Additionally, the use of high doses of CQ may cause severe toxicity, especially when combined with other chemotherapeutic agents due to its nephrotoxicity [19,20]. Recent attempts have focused on the discovery of more potent CQ analogs that could inhibit autophagy at lower concentrations [21,22]. Biaminoquinoline analogs were reported to be superior to CQ in inhibiting autophagy through enhanced lysosomotropic effects [23]. In this study, we initially hypothesized that the design of bivalent CQ analogs that utilized a piperazinyl-based polyamine-like linker could enhance CQ potency due to enhanced lysosomal accumulation through the polyamine transporter. Interestingly, the most potent compounds identified in this series (Figure 1) were found to act as autophagy inducers rather than inhibitors [7].

Materials and Methods

Protocols for Biological Assays

The cell line, MDA-MB-231 (Cat. #: CRM-HTB-26) was purchased from ATCC (Manassas, VA, USA). The cells were grown using RPMI 160 media (Gibco, Cat. #: 11875093) supplemented with 10% FBS and 1% penicillin/streptomycin (Thermo-Fisher, Grand Island, NY, USA). The antibodies LC3B-II (Cat. #: 3868S) was obtained from cell signaling technologies (Danvers, MA, USA). Antibodies to GAPDH (Cat. #: SC25778) and p62 (Cat. #: SC28359) were purchased from Santa Cruz Biotechnology (Dallas, TX, USA). Bafilomycin A1 (Cat. #: B1793) was purchased from Sigma Aldrich (St. Louis, MO, USA). Non-radioactive cell titer assay (Cat. #: G4100) and Apo-One homogenous caspase 3/7 assay (Cat. #: G7790) were purchased from Promega (Madison, WI, USA).

Cell Viability Assays

MDA-MB-231 cells were plated in 96-well plates at a density of 4000 cells/well. The cells were treated with the indicated compound concentrations for 48 hours followed by assessment of cell viability using MTT assay.

*Address for Correspondence: Yasser Heikal, Department of Pharmaceutical, Social and Administrative Sciences, School of Pharmacy, D'Youville College, 320 Porter Ave., Buffalo, NY 14201, E-mail: heakaly@dyc.edu

Copyright: © 2020 Heikal Y, et al. This is an open-access article distributed under the terms of the creative commons attribution license which permits unrestricted use, distribution and reproduction in any medium, provided the original author and source are credited.

Received 25 January, 2020; Accepted 05 February, 2020; Published 13 February, 2020

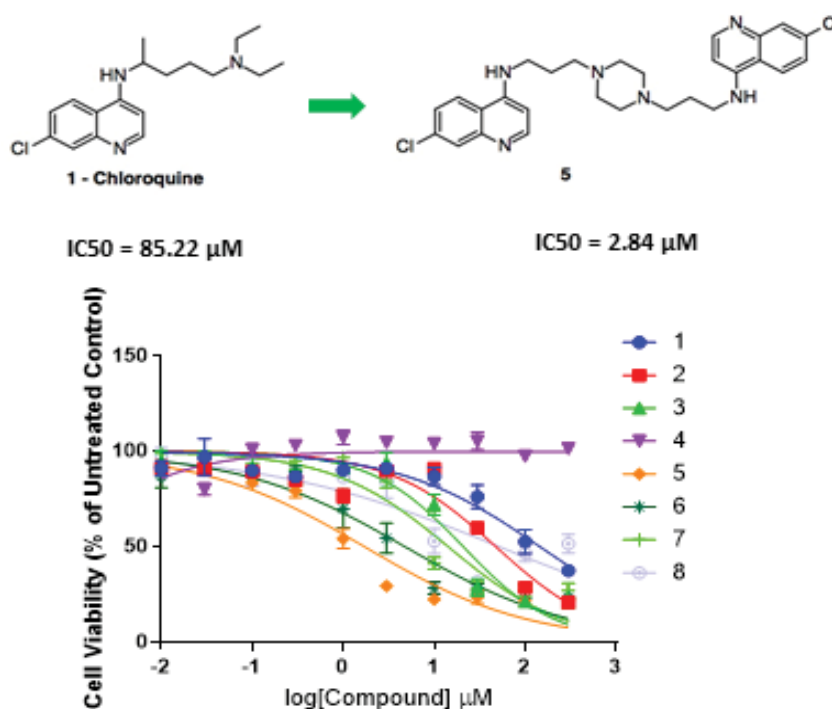


Figure 1. The chloroquine analog, compound 5, with improved cytotoxicity in MDA-MB-231 cells.

Caspase 3/7 Activity Assays

MDA-MB-231 cells were plated in 96-well plates at a density of 4000 cells/well. The cells were treated with the indicated compound concentrations for 24 hours followed by assessment of caspase 3/7 activity using homogenous apo caspase 3/7 activity assay.

Western Blot Analysis of LC3B-II and p62 Proteins

MDA-MB-231 cells were plated in 6-well plates and were treated with the indicated compound concentration at confluence of 80%. Following 24 hours, total protein was harvested using CellLytic M buffer (Cat.# C2978) obtained from MilliporeSigma (Burlington, MA) supplemented with protease inhibitor cocktail. Total protein was analyzed using western blotting and the images were produced using FluorChem M imager (Cell Biosciences, Inc., San Jose, CA, USA). Densitometry was performed using ImageJ software (NIH, Bethesda, MD, USA).

Statistical Analysis

Data were analyzed using Graphpad Prism software (GraphPad Prism Inc., La Jolla, CA, USA). Statistical significance of the data was determined using Students' t-test, one-way, or two-way ANOVA analysis, as appropriate.

Chemistry

The compounds were synthesized following literature methods as shown in Schemes 1 and 2 [24-29]. All reagents were used as received from commercial suppliers unless otherwise stated. Flash chromatography was performed on silica gel (32-63D 60 Å) according to the method of Still [30]. Thin layer chromatography (TLC) was performed on aluminum backed plates pre-coated with silica (0.25 mm, 60F-254) which were developed using standard visualizing agents: UV fluorescence (254 and 366 nm). ¹H NMR spectra were recorded on a Bruker Avance III HD 400 FT Nuclear Magnetic Resonance spectrometer. The following abbreviations apply: (b) broad, (s) singlet, (d) doublet, (t) triplet, (q) quartet, (m) multiplet, (dd) doublet doublet, etc. Chemical shifts are given in ppm. *J* values are recorded in Hz and are rounded to the nearest tenth.

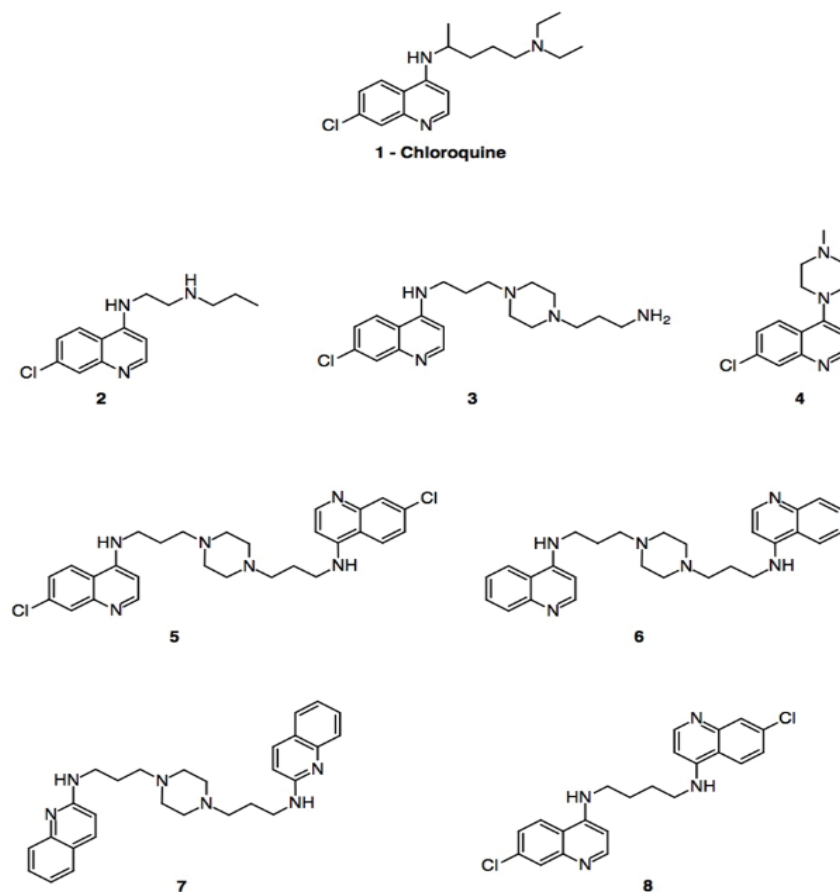
7-Chloro-N-(2-propylamino)ethyl)quinoline-4-amine HCl (2)

Synthesized following the literature method [24-26]. 4,7-dichloroquinoline

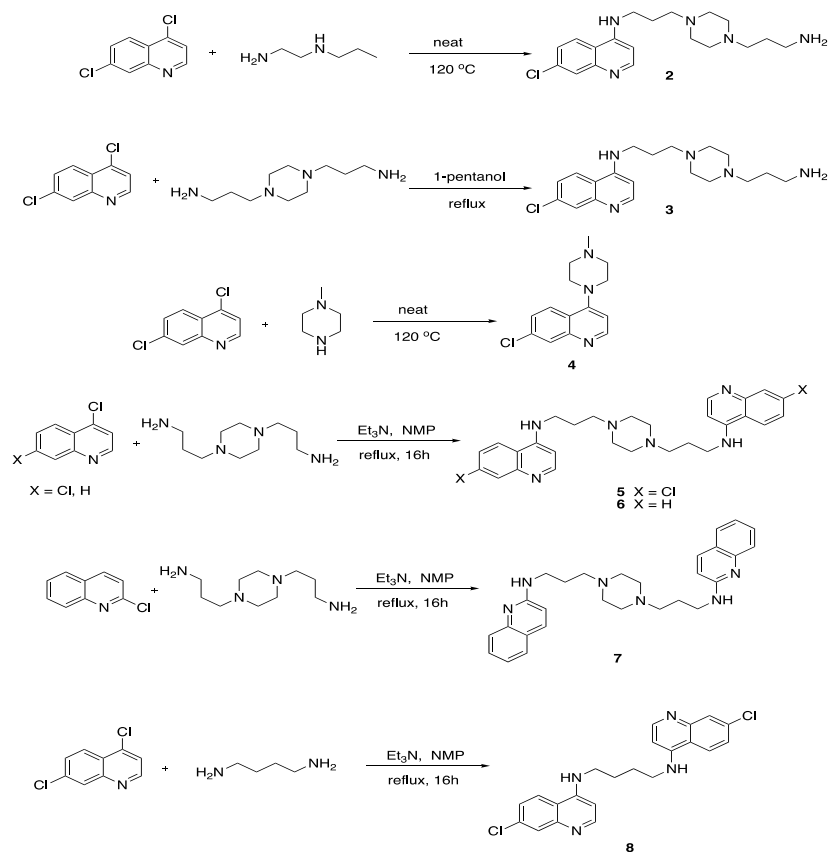
(1.02 g, 5.1 mmol, 1.0 equiv) and *N*-propylethylenediamine (1.58 g, 15.44 mmol, 3.0 equiv) were added to a 100 mL flask and heated to 120 °C for four hours under argon. After cooling to room temperature, added about 10 mL of 1.0 M NaOH solution in water and extracted with dichloromethane (DCM) (5 × 15 mL). Filtered off the insoluble solid and dried the organic phase with Na₂SO₄. Concentrated *in vacuo* to a yellow solid. The solid was purified via column chromatography using 90:9:1 DCM/MeOH/NH₄OH to give a pale yellow solid. R_f=0.21 (MeOH/DCM/NH₄OH) Yield: 1.04 g (77%). The product was dissolved in 5 mL of ethanol and added 6 mL of 6.0 M HCl in ethanol. Stirred overnight and filtered off the product as a white solid. m. p. 274-281 °C decomp. ¹H NMR (400 MHz, D₂O) δ 8.35 (d, *J*=6.8 Hz, 1H), 8.05-8.03 (m, 1H), 7.72 (m, 1H), 7.56-7.54 (m, 1H), 6.83 (d, 7.2 Hz, 1H), 3.95 (t, *J*=6.0 Hz, 2H), 3.44 (t, *J*=6.0 Hz, 2H), 3.06 (dd, *J*=8.8 Hz, *J*=7.6 Hz, 2H), 1.70 (sextet, *J*=7.6 Hz, 1H), 0.94 (t, *J*=7.2 Hz, 2H). ¹³C NMR (100 MHz, D₂O) δ 156.0, 142.8, 139.6, 137.8, 127.8, 124.1, 119.0, 115.2, 98.6, 49.7, 45.0, 39.4, 19.1, 10.2. IR (neat) 3377, 3177, 3098, 3016, 2933, 2712, 2526, 2423, 1633, 1608, 1590, 1557, 1455, 1423, 1385, 1363, 1305, 1266, 1247, 1218, 1165, 1143, 1090, 1045, 1017, 959, 898, 813, 799, 762, 674, 662, 603, 589 cm⁻¹. HRMS (ESI) Calcd. for C₁₄H₁₉ClN₃: 264.12620. Found: 264.12641.

N-3- 4-(3-aminopropyl)piperazin-1-yl)propyl)-7-chloroquin-4-amine HCl (3)

Synthesized following the literature method [27]. 4,7-dichloroquinoline (1.02 g, 5.0 mmol, 1.0 equiv) and 1,4-bis (3-aminopropyl)piperazine (1.03 g, 5.0 mmol, 1.0 equiv) were added to a 100 mL flask in 1-pentanol and heated to reflux for 18 hours under argon. After cooling to room temperature, added about 10 mL of 1.0 M NaOH solution in water and extracted with DCM (5 × 15 mL). Filtered off the insoluble solid and dried the organic phase with Na₂SO₄. Concentrated *in vacuo* to a yellow oil. The crude product was purified via column chromatography using 80:19:1 DCM/MeOH/NH₄OH to give a pale yellow oil. R_f=0.51 (MeOH/DCM/NH₄OH), Yield: 0.8505 g (47%). Then dissolved 0.1751 g of the product was dissolved in 6.0 M HCl in water and 10 mL of ethanol. Stirred overnight and filtered off the solid to give a pale tan solid. m. p. 286-288 °C decomp. ¹H NMR (400 MHz, D₂O) δ 8.26 (m, 1H), 7.99 (m, 1H), 7.68 (m, 1H), 7.51 (m, 1H), 6.77-6.75 (m, 1H), 3.73-3.67 (m, 10H), 3.48-4.47 (m, 4H), 3.10-3.06 (m, 2H), 2.26-2.14 (m, 4H). ¹³C NMR (100 MHz, D₂O) δ 155.6, 142.3, 139.3, 137.5, 127.4, 123.9, 118.8, 114.8, 98.5, 54.4, 53.7, 48.9 (4-C), 40.2, 36.4, 22.5, 21.8. IR (neat) 3345, 2953, 2795, 1613, 1591, 1553, 1420, 1407, 1353, 1337, 1277, 1248, 1080, 1015, 956, 905, 891, 812, 768, 653 cm⁻¹. HRMS (ESI) Calcd. for C₁₉H₂₉ClN₅: 362.21060. Found: 362.21062.



Scheme 1. Structure of CQ analogs.



Scheme 2. Synthesis of CQ analogs.

7-chloro-4- (4-methylpiperazin-1-yl)quinoline (4)

4,7-dichloroquinoline (1.01 g, 5.0 mmol, 1.0 equiv) and 1-methylpiperazine (2.52 g, 25.2 mmol, 5.0 equiv) were added to a 100 mL flask and heated to 120 °C for four hours under argon. After cooling to room temperature, added about 10 mL of 1.0 M NaOH solution in water and extracted with DCM (5 × 15 mL). Filtered off the insoluble solid and dried the organic phase with Na₂SO₄. Concentrated *in vacuo* to a yellow solid. The solid was purified via column chromatography using 90:9:1 MeOH/DCM/NH₄OH, Yield: 1.07 g (82%). m. p. 83-86°C. ¹H NMR (400 MHz, D₂O) δ 8.71 (d, J=5.2 Hz, 1H), 8.03 (d, J=2.0 Hz, 1H), 7.94 (d, J=9.2 Hz, 1H), 7.42 (dd, J=8.8 Hz, J=2.0 Hz, 1H), 6.84 (d, J=5.2 Hz, 1H), 2.54 (m, 4H), 2.71 (m, 4H), 2.42 (s, 3H). ¹³C NMR (100 MHz, D₂O) δ 156.9, 151.9, 150.2, 134.8, 128.9, 126.1, 125.2, 121.9, 109.0, 55.0, 52.1, 46.1. IR (neat) 3040, 2968, 2937, 2830, 2793, 2765, 1610, 1573, 1563, 1495, 1458, 1419, 1370, 1298, 1284, 1251, 1238, 1138, 1007, 925, 868, 838, 824, 775, 654 cm⁻¹. HRMS (ESI) Calcd. for C₁₄H₁₇ClN₃: 262.11055. Found: 262.11052.

7-chloro-N- (3- (4- (3- (7-chloroquinolin-4-ylamino)propyl)piperazin-1-yl)propyl)quinoline-4-amine HCl (5)

Synthesized as described in the literature [28,29]. 4,7-dichloroquinoline (1.98 g, 10.0 mmol, 2.0 equiv) and 1,4-bis (3-aminopropyl)piperazine (1.0016 g, 5.0 mmol, 1.0 equiv) and triethylamine (1.4 mL, 10 mmol, 2.0 equiv) were added to 10 mL of N-methylpyrrolidinone and heated to reflux for 16 hours. Filtered off the light tan solid. Yield: 2.199 g (84%). 0.1911 g of product was added to 10 mL of 6.0 M HCl in water and 10 mL of ethanol. Stirred overnight and filtered off the product as a white solid. m.p. 280°C (decomp). ¹H NMR (400 MHz, D₂O) δ 8.28 (d, J=7.2 Hz, 2H), 8.07 (d, J=9.2 Hz, 2H), 7.77 (d, J=2.0 Hz, 2H), 7.57 (dd, J=8.8 Hz, 2.0 Hz, 2H), 6.78 (d, J=7.2 Hz, 2H), (3.69-3.61 (m, 12H), 3.40-3.36 (m, 4H), 2.24-2.20 (m, 4H). ¹³C NMR (100 MHz, D₂O) δ 155.8, 142.4, 139.4, 137.7, 127.5, 124.0, 118.9, 115.0, 98.4, 54.4, 49.0, 40.2, 22.6. IR (neat) 3233, 2431, 1607, 1559, 1447, 1354, 1237, 1215, 1142, 1078, 1027, 967, 866, 812, 761, 655 cm⁻¹. HRMS (ESI) Calcd for C₂₈H₃₃Cl₂N₆: 523.21383. Found: 523.21370.

N- (3- (4- (3- (quinoline-4-ylamino)propyl)piperazin-1-yl)propyl)quinoline-4-amine HCl (6)

7-chloroquinoline (1.027 g, 6.28 mmol, 2.0 equiv) and 1,4-bis (3-aminopropyl)piperazine (0.63 g, 3.14 mmol, 1.0 equiv) and triethylamine (0.9 mL, 6.28 mmol, 2.0 equiv) were added to 10 mL of N-methylpyrrolidinone and heated to reflux for 16 hours. Filtered off the white solid. Yield: 1.1092 g (71%). The product was added to 10 mL of 6.0 M HCl in water and 10 mL of ethanol. Stirred overnight and filtered off the product as a white solid. m. p. 282-283°C (decomp). ¹H NMR (400 MHz, D₂O) δ 8.25 (d, J=7.2 Hz, 2H), 8.09 (d, J=7.6 Hz, 2H), 7.84 (dd, J=8.0 Hz, J=6.8 Hz, 2H), 7.73 (d, J=8.4 Hz, 2H), 7.60 (dd, J=8.0 Hz, J=6.8 Hz, 2H), 6.73 (d, J=7.2 Hz, 2H), 3.66-3.56 (m, 12H), 3.39-3.35 (m, 4H), 2.23-2.15 (m, 4H). ¹³C NMR (100 MHz, D₂O) δ 156.2, 141.8, 137.4, 133.7, 127.1, 122.1, 120.0, 116.8, 97.9, 54.4, 49.0, 39.9, 22.6. IR (neat) 3247, 2803, 1619, 1593, 1553, 1471, 1450, 1418, 1355, 1256, 1229, 1125, 951, 885, 763, 664 cm⁻¹. HRMS (ESI) Calcd. for C₂₈H₃₅N₆: 455.29177. Found: 455.29179.

N- (3- (4- (3- (quinoline-2-ylamino)propyl)piperazin-1-yl)propyl)quinoline-2-amine HCl (7)

2-chloroquinoline (1.2488 g, 7.63 mmol, 2.0 equiv) and 1,4-bis (3-aminopropyl)piperazine (0.7648 g, 3.82 mmol, 1.0 equiv) and triethylamine (1.1 mL, 6.28 mmol, 2.0 equiv) were added to 10 mL of N-methylpyrrolidinone and heated to reflux for 24 hours. Filtered off the white solid. Yield: 0.7026 g (41%). The product was added to 10 mL of 6.0 M HCl in water and 10 mL of ethanol. Stirred overnight and filtered off the product as a white solid. m. p. 289-291°C (decomp). ¹H NMR (400 MHz, D₂O) δ 8.21 (m, 2H), 7.83 (d, J=7.6 Hz, 2H), 7.75 (d, J=4.0 Hz, 4H), 7.50 (m, 2H), 7.02 (m, 2H), 3.66-3.58 (m, 12H), 3.34 (m, 4H), 2.23-2.16 (m, 4H). ¹³C NMR (100 MHz, D₂O) δ 152.8, 142.9, 135.7, 132.8, 128.8, 125.7, 121.4, 117.2, 114.0, 54.2, 49.2, 39.1, 22.9. IR (neat) 3006, 1660, 1444, 1128, 952, 826, 766, 598 cm⁻¹. HRMS (ESI) Calcd. for C₂₈H₃₅N₆: 455.29177. Found: 455.29227.

7-chloro-N- (4- (7-chloroquinolin-4-ylamino)butyl)quinoline-4-amine HCl (8)

4,7-dichloroquinoline (1.98 g, 10 mmol, 2.0 equiv) and butane diamine (0.4408 g, 5 mmol, 1.0 equiv) and triethylamine (1.4 mL, 10 mmol, 2.0 equiv) were added to 10 mL of N-methylpyrrolidinone and heated to reflux for 16 hours. Filtered off the brown solid product. Yield: 1.76 g (62%). Dissolved the product in 10 mL of 6.0 M HCl in water and 10 mL of ethanol. Stirred overnight and filtered off the solid to give a tan solid. m.p. 195-200°C (decomp). ¹H NMR (400 MHz, D₂O) δ 8.05-8.02 (m, 1H), 7.52-7.44 (m, 2H), 7.31-7.29 (m, 1H), 6.67-6.64 (m, 1H), 3.53 (s, 2H), 1.91 (s, 2H). ¹³C NMR (100 MHz, D₂O) δ 155.0, 141.7, 139.2, 137.0, 127.1, 122.7, 118.6, 114.7, 98.6, 42.3, 22.3. IR (neat) 3228, 3104, 3020, 2852, 2821, 1611, 1589, 1564, 1448, 1358, 1243, 1214, 1165, 1141, 1026, 904, 873, 817, 788, 762, 650 cm⁻¹. HRMS (ESI) Calcd. for C₂₂H₂₁Cl₂N₄: 411.11378. Found: 411.11313.

Results and Discussion

Anticancer activity in breast cancer cells

The cytotoxic activity of the synthesized compounds was assessed in MDA-MB-231 breast cancer cell line using 3- (4,5-Dimethylthiazol-2-yl)-2,5-diphenyltetrazolium bromide (MTT) assay (Figure 2). The IC₅₀ of CQ (1) was found to be 85.22 μM. Modifying the side chain on position 4 of the quinoline ring as shown in compound 2 resulted in slight enhancement of the anticancer activity with IC₅₀ of 66.53 μM. We then decided to explore the effect of incorporating a piperazinyl group, which would enhance aqueous solubility. The addition of piperazinyl group as shown in compound 3 resulted in significant enhancement of the cytotoxic activity with an IC₅₀ of 22.14 μM. However, direct attachment of the piperazinyl group as shown in compound 4 resulted in the loss of the anticancer activity which may suggest that the presence of the amine-based linker is required for the compound activity. Several groups have reported the design of bivalent chloroquine analogs with enhance cytotoxicity and improved autophagy inhibitory activity [23]. Therefore, we decided to use the piperazinyl group as a building block as it offers the advantage of easy access to the chloroquine bivalent analogs. We decided to explore this strategy by synthesizing compound 5. Interestingly, the IC₅₀ of compound 5 was found to be 2.84 μM. To further characterize the structure activity relationship of compound 5, we synthesized compound 6 that lacks Cl groups on position 7 of the quinoline ring. Interestingly this modification resulted in slight increase in the IC₅₀ 5.98 μM. However, changing the location of the linker from position 4 to position 2 as shown in compound (7) resulted in significant increase in the IC₅₀ to 14.04 μM. This suggest that compound 5 activity could be mediated through specific protein interaction event that requires specific unique structural features that are present in compound 5 and are lost upon changing the location of the linker on the quinoline ring. The importance of the piperazinyl group was further established by making the bivalent compound 8 which lacks the piperazinyl group. This modification resulted in loss of potency as evident by the IC₅₀ of about 52 μM additionally; compound 8 had limited aqueous solubility. This could be due to the ability of the piperazinyl group to facilitate binding to a specific target, or it could be also due to the length of the linker that connects the two quinoline groups and facilitate specific interaction with protein target (s). Additionally, it could be possible that the activity is in part dependent upon utilizing the polyamine transporter that might enhance compounds cellular accumulation in cancer cells.

The compound effects on autophagy and apoptosis: To determine the effect of the CQ analogs on autophagic flux, the levels of LC3B-II, a protein marker for autophagy, and p62, another widely used protein marker that undergoes autophagy-dependent degradation, were analyzed using western blotting (Figure 3). Treatment of MDA-MB-231 cells with 5 μM CQ, 3, 5, 6 or 7 resulted in increase in the level of LC3B-II. Notably, compounds 5 and 6 resulted in about 6 times increase in the level of LC3B-II and complete disappearance of LC3B-I which may suggest that these compounds are inducing rather than inhibition autophagic flux (Figure 3B). To confirm this hypothesis, we examined the level of p62 protein which undergoes autophagy-dependent degradation [31]. Interestingly, treatment with compounds 5 and 6 resulted in significant degradation of p62 (Figure 3C) which confirms that these

compounds induce, rather than inhibit autophagic flux. Compound 5 was more effective p62 degrader relative to compounds 6 and 7 which indicate that the chlorine atoms and the location of the piperazinyl linker on the quinoline ring play a key role in this molecular effect. Additionally, we analyzed the ratios of LC3B-I/LC3B-II (Figure 3D), which also suggest that compounds 5, 6 and 7 significantly reduce the level of LC3-I while enhance the expression of LC3B-II when compared with chloroquine, suggesting unique effects on the autophagic flux that involves induction.

To determine if the CQ analogs were inducing apoptotic cell death, we analyzed caspase 3/7 activity (Figure 4). MDA-MB-231 cells were treated with CQ, 3, 5, 6 and 7 at concentration of 5 and 10 μ M. Interestingly, at 5 μ M concentration, compound 5 was the only analog to robustly induced caspase 3/7 activity (about 2-fold increase). At 10 μ M concentration, compound 5 was the only analog to robustly induced caspase 3/7 activity (about one-fold increase). To assess the role of autophagy induction in the observed apoptotic cell death, we treated MDA-MB-231 cells with compound 5 in the presence or absence of bafilomycin A1, known autophagy inhibitor that suppress autophagy through inhibition of V-ATPase. Interestingly, bafilomycin A1 treatment blocked compound 5 induced apoptosis (Figure 5A). Additionally,

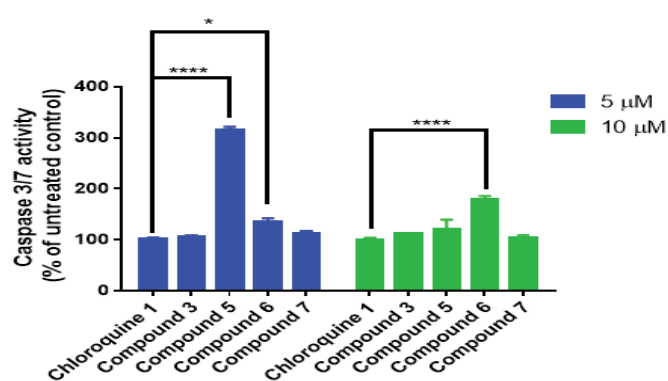


Figure 4. The effect of CQ analogs on caspase 3/7 activity. MDA-MB-231 cells were treated with the indicated compound concentration for 24 hours followed by assessment of caspase 3/7 activity. Error bars represent \pm SEM of at least 2 independent experiments.

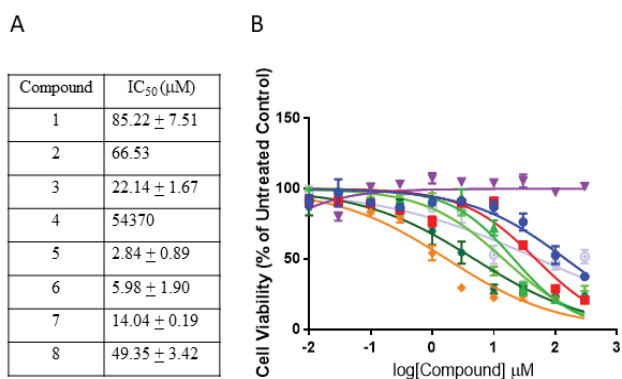


Figure 2. Structure activity relationship of the CQ analog series. A. IC₅₀ values were measured in MDA-MB-231 cells at 48 hrs timepoints and cell viability was assessed using MTT assay. B. Dose response curves were generated using GraphPad prism. Error bars represent \pm SEM of at least 4 replicates.

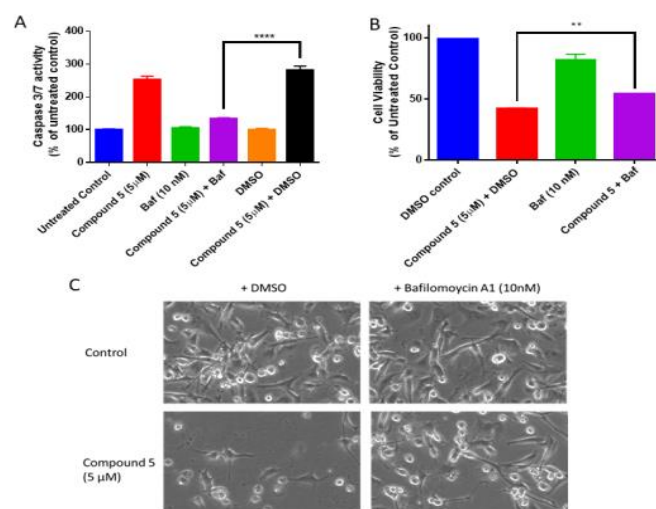


Figure 5. The effect of the autophagy inhibitor bafilomycin A1 on the activity of compound 4. (A) MDA-MB-21 cells were treated with compound 4 (5 μ M) in the presence or absence of 10 nM bafilomycin A1 for 24 hours. Caspase 3/7 activity was assessed using Apo-One homogenous caspase 3/7 assay; error bars represent \pm SEM. (B) MDA-MB-231 cells were treated with compound 3 in the presence or absence of bafilomycin A1 and cell viability was assessed 24 hours post treatment using MTT cell viability assay. Error bars represent \pm SEM. (C) MDA-MB-231 cells were treated with compound 4 in the presence or absence of bafilomycin A1 and cell pictures were taken using 10X magnification; representative picture of N=3 experiments. The data represent at least N=3 experiments.

bafilomycin A1 treatment resulted in partial rescue of cell viability, suggesting possible involvement of other cell death mechanisms (Figures 5B and 5C). Collectively, these results suggest that autophagy induction by compound 5 plays a significant part in induction of apoptotic cell death.

Future studies will focus on the analysis of the molecular mechanisms involved in compound 5-induced cell death and the mechanism of autophagy induction to further develop more potent autophagy modulators with the potential to advance into the clinic. Additionally, the potential selectivity of these new analogs for specific breast cancer subtype (s) is currently under investigation.

Conclusion

Collectively, the data presented demonstrate the development of more potent chloroquine analogues that could modulate autophagic flux at much lower concentrations. Interestingly, the most potent analogs identified in our series induced autophagic flux. Furthermore, translation of these analogs may yield compounds that could be administered at lower concentrations with reduced adverse events. Several structural features may contribute to the enhanced potency. The incorporation of the polyamine moiety may enhance the compound uptake by the cancer cells relative to normal cells

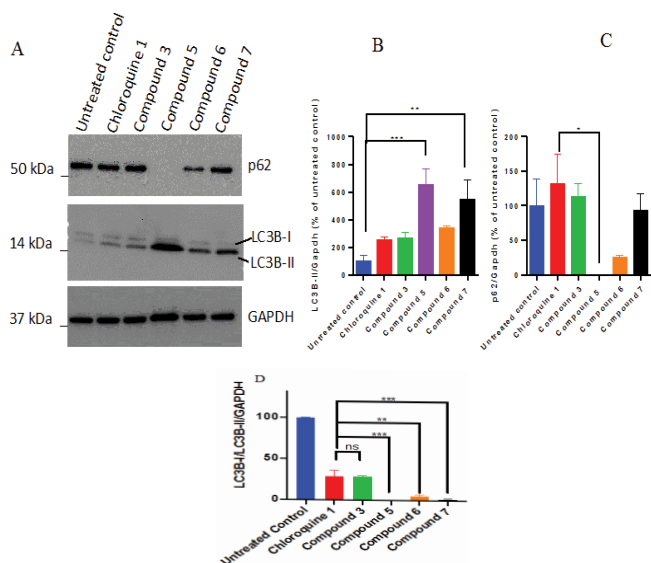


Figure 3. The effect of CQ analogs on autophagic flux. (A) MDA-MB-231 cells were treated with the indicated compounds at 5 μ M concentrations for 24 hours, followed by protein analysis using western blotting. Quantification of the level of LC3B-II and p62 following compound treatment are presented. (B) Quantification of the expression level of LC3B-II. (C) Quantification of the expression level of p62. (D) Quantification of the ratios of LC3B-I/LC3B-II/GAPDH. Error bars represent SEM of at least 3 independent experiments. Representative blots of at least 3 independent experiments. Error bars represent \pm SEM.

[32,33]. Several studies indicated that cancer cells require higher polyamine levels for growth and survival. Another possible unique aspect is the ability of these compounds to accumulate into the lysosomes, which could result in more potent effects on autophagic flux. Future studies will focus on defining the mechanism of autophagy induction by these compounds and whether they induce canonical and/or non-canonical forms of autophagy.

Author Contributions

YH and DV wrote and edited the manuscript. YH designed and conducted the biological experiments, analyzed the data. DV designed synthesized and characterized compounds. DP synthesized and characterized compounds, conducted biological experiments, analyzed the data and synthesized and characterized compounds. PC and AO conducted biological experiments and analyzed the data. CL synthesized and characterized compounds. All authors have given approval to the final version of the manuscript.

Funding

This research was supported by funds from the School of Pharmacy and D'Youville College, American Society for Pharmacology, Experimental Therapeutics (ASPET), The Department of Chemistry and the research committee at D'Youville College.

Acknowledgments

The authors would like to acknowledge the American Association for Pharmacology and Experimental Therapeutics (ASPET) funding which supported a Summer Research Fellowship (SURF) award to Dhvani Patel to participate in the research project. We would also like to thank the Department of Chemistry and the Research Committee at D'Youville College for the funding of this project. We would also like to thank Buffalo State College for their generosity in the use of their NMR spectrometer.

Conflicts of Interest

The authors declare no conflict of interest.

References

- Onorati, Angelique V, Matheus Dyczynski, Rani Ojha, and Ravi K. Amaravadi. "Targeting autophagy in cancer." *Cancer* 124 (2018): 3307-3318.
- Kumar, Ankit, Umesh Kumar Singh, and Anurag Chaudhary. "Targeting autophagy to overcome drug resistance in cancer therapy." *Future Med Chem* 7 (2015): 1535-1542.
- Cheng, Yan, Xingcong Ren, William N. Hait, and Jin-Ming Yang et al. "Therapeutic targeting of autophagy in disease: biology and pharmacology." *Pharmacol Rev* 65 (2013): 1162-1197.
- Condello, Maria, Evelin Pellegrini, Michele Caraglia, and Stefania Meschini, et al. "Targeting autophagy to overcome human diseases." *Int J Mol Sci* 20 (2019): 725.
- Karantza-Wadsworth, Vassiliki, Shyam Patel, Olga Kravchuk, and Guanghua Chen, et al. "Autophagy mitigates metabolic stress and genome damage in mammary tumorigenesis." *Genes Dev* 21 (2007): 1621-1635.
- Lefort, Sylvain, Carine Joffre, Yann Kieffer, and Anne-Marie Givel, et al. "Inhibition of autophagy as a new means of improving chemotherapy efficiency in high-LC3B triple-negative breast cancers." *Autophagy* 10 (2014): 2122-2142.
- Rodriguez, Cristina E., Sara I. Reidel, Elisa D. Bal de Kier Joffe, and Maria A. Jasniz, et al. "Autophagy protects from trastuzumab-induced cytotoxicity in HER2 overexpressing breast tumor spheroids." *PLoS One* 10 (2015).
- Vijayaraghavan, Smruthi, Cansu Karakas, Iman Doostan, and Xian Chen, et al. "CDK4/6 and autophagy inhibitors synergistically induce senescence in Rb positive cytoplasmic cyclin E negative cancers." *Nat Commun* 8 (2017): 1-17.
- Cook, Katherine L., Ayesha N. Shajahan, and Robert Clarke. "Autophagy and endocrine resistance in breast cancer." *Expert Rev Anticancer Ther* 11 (2011): 1283-1294.
- Han, Myung Woul, Jong Cheol Lee, Jun-Young Choi, and Gui Chul Kim, et al. "Autophagy inhibition can overcome radioresistance in breast cancer cells through suppression of TAK1 activation." *Anticancer Res* 34 (2014): 1449-1455.
- Maycotte, Paola, and Andrew Thorburn. "Targeting autophagy in breast cancer." *World J Clin Oncol* 5 (2014): 224.
- Maycotte, Paola, Christy M. Gearheart, Rebecca Barnard, and Suraj Aryal, et al. "STAT3-mediated autophagy dependence identifies subtypes of breast cancer where autophagy inhibition can be efficacious." *Cancer Res* 74 (2014): 2579-2590.
- Masso-Welch, Patricia, Sofia Giraldo Berlingeri, Natalie D. King-Lyons, and Lorrie Mandell, et al. "LT-IIc, a bacterial type II heat-labile enterotoxin, induces specific lethality in triple negative breast cancer cells by modulation of autophagy and induction of apoptosis and necroptosis." *Int J Mol Sci* 20 (2019): 85.
- Luna-Dulcey, Liany, Rebeka Tomasin, Marina A. Naves, James A. da Silva, and Marcia R. Cominetti. "Autophagy-dependent apoptosis is triggered by a semi-synthetic [6]-gingerol analogue in triple negative breast cancer cells." *Oncotarget* 9 (2018): 30787.
- Akimoto, Miho, Mari Iizuka, Rie Kanematsu, and Masato Yoshida, et al. "Anticancer effect of ginger extract against pancreatic cancer cells mainly through reactive oxygen species-mediated autotic cell death." *PLoS One* 10 (2015): e0126605.
- Liu, Y., and Beth Levine. "Autosis and autophagic cell death: the dark side of autophagy." *Cell Death Differ* 22 (2015): 367-376.
- Mauthe, Mario, Idil Orhon, Cecilia Rocchi, and Xingdong Zhou, et al. "Chloroquine inhibits autophagic flux by decreasing autophagosome-lysosome fusion." *Autophagy* 14 (2018): 1435-1455.
- Chude, Cynthia I., and Ravi K. Amaravadi. "Targeting autophagy in cancer: update on clinical trials and novel inhibitors." *Int J Mol Sci* 18 (2017): 1279.
- Kimura, Tomonori, Yoshitsugu Takabatake, Atsushi Takahashi, and Yoshitaka Isaka. "Chloroquine in cancer therapy: a double-edged sword of autophagy." *Cancer Res* 73 (2013): 3-7.
- Takahashi, Atsushi, Tomonori Kimura, Yoshitsugu Takabatake, and Tomoko Namba, et al. "Autophagy guards against cisplatin-induced acute kidney injury." *Am J Pathol* 180 (2012): 517-525.
- He, Siyu, Qi Li, Xueyang Jiang, and Xin Lu, et al. "Design of small molecule autophagy modulators: a promising druggable strategy." *J Med Chem* 61 (2017): 4656-4687.
- Amaravadi, Ravi K., and Jeffrey D. Winkler. "Lys05: A new lysosomal autophagy inhibitor." *Autophagy* 8 (2012): 1383-1384.
- McAfee, Quentin, Zhihui Zhang, Arabinda Samanta, and Samuel M. Levi, et al. "Autophagy inhibitor Lys05 has single-agent antitumor activity and reproduces the phenotype of a genetic autophagy deficiency." *Proc Natl Acad Sci* 109 (2012): 8253-8258.
- Natarajan, Jayakumar K., John N. Alumasa, Kimberly Yearick, and Kekeli A. Ekoue-Kovi, et al. "4-N-, 4-S-, and 4-O-chloroquine analogues: influence of side chain length and quinolyl nitrogen p Ka on activity vs chloroquine resistant malaria." *J Med Chem* 51 (2008): 3466-3479.
- Musonda, Chitalu C, Jiri Gut, Philip J. Rosenthal, and Vanessa Yardley. "Application of multicomponent reactions to antimalarial drug discovery. Part 2: new antiplasmodial and antitypanosomal 4-aminoquinoline γ - and δ -lactams via a 'catch and release' protocol." *Bioorg Med Chem* 14 (2006): 5605-5615.

26. Lekostaj, Jacqueline K., Jayakumar K. Natarajan, Michelle F. Paguio, and Christian Wolf, et al. "Photoaffinity Labeling Of The Plasmodium Falciparum Chloroquine Resistance Transporter with a Novel Perfluorophenylazido Chloroquine." *Biochemistry* 47 (2008): 10394-10406.
27. Ryckebusch, Adina, Rébecca Deprez-Poulain, Louis Maes, and Marie-Ange Debreu-Fontaine, et al. "Synthesis and In vitro and In vivo Antimalarial Activity of N-(7-Chloro-4-quinoly)-1,4-bis(3-aminopropyl) piperazine Derivatives." *J Med Chem* 46 (2003): 542-557.
28. Vennerstrom, Jonathan L., Hong Ning Fu, William Y. Ellis, and Arba L, et al. Milhous. "Dispiro-1, 2, 4, 5-tetraoxanes: a new class of antimalarial peroxides." *J Med Chem* 35 (1992): 3023-3027.
29. Tewari, Swati, Chauhan Pam, Bhaduri A.P., and Nigar Fatima, et al. "Syntheses and antifilarial profile of 7-chloro-4- (substituted amino) quinolines: A new class of antifilarial agents." *Bioorg Med Chem Lett* 10 (2000): 1409-1412.
30. Still, W. Clark, Michael Kahn, and Abhijit Mitra. "Rapid chromatographic technique for preparative separations with moderate resolution." *J Org Chem* 43 (1978): 2923-2925.
31. Bjørkøy, Geir, Trond Lamark, Serhiy Pankiv, and Aud Overvatn et al. "Monitoring autophagic degradation of p62/SQSTM1." *Methods Enzymol* 452 (2009): 181-197.
32. Wang, Chaojie, Jean-Guy Delcros, John Biggerstaff, and Otto Phanstiel IV. "Molecular requirements for targeting the polyamine transport system. Synthesis and biological evaluation of polyamine-anthracene conjugates." *J Med Chem* 46 (2003): 2672-2682.
33. Roy, Upal K. Basu, Nathaniel S. Rial, Karen L. Kachel, and Eugene W. Gerner. "Activated K-RAS increases polyamine uptake in human colon cancer cells through modulation of caveolar endocytosis." *Mol Carcinog* 47 (2008): 538-553.

How to cite this article: Heakal Y, Patel D, Cao P, and Lincourt CC, et al. "Discovery of Autophagy-Inducing Chloroquine Analogs with Potent Anticancer Activity in Breast Cancer Cells." *Med Chem (Los Angeles)* 10 (2020). doi: 10.37421/mccr.2020.10.543